

Center of Mass Estimation in Irregular Planar Terrains using a Geometric Approach

Luenin Barrios and Wei-Min Shen

Abstract—Locomotion maneuvers over irregular terrains involve complex forces and movements that make estimation of center of mass(CoM) behavior a challenging task. Nevertheless, understanding CoM dynamics remains pivotal in locomotion planning for both humans and robots. Current methods for CoM position estimation rely heavily on expensive and ungainly tools, for example force plates, that render CoM analysis impractical and time consuming. To tackle these challenges, this paper proposes an efficient and reliable geometric approach for CoM estimation that delivers accurate CoM behavior in irregular planar terrains. The geometric approach depends only on terrain geometry information and essential kinematic data of the moving body. Using this key information in conjunction with an Optimized Geometric Hermite(OGH) curve, a model is developed that produces accurate CoM position and phase space behavior. Various human case studies were analyzed to validate the effectiveness of the approach. The results show that for natural walking over irregular planar terrains, the geometric approach generates accurate CoM path approximations and state space trajectories and is a powerful tool for understanding CoM position in irregular planar terrains.

I. INTRODUCTION

Accurate prediction and modeling of CoM behavior is fundamentally important in developing motion planners that are faithful to the CoM dynamics observed in the real world. This necessity is paramount to robot motion planners aiming for performance equivalence with human locomotion. Human locomotion is extremely varied and replete with complex force interactions that makes CoM study very difficult. The problem is further exacerbated when the immensity of terrains is considered. Planar and non-planar terrains affect CoM behavior in uniquely different ways and introduce additional parameters that must be addressed by the motion planner. Despite these challenges, CoM estimation remains central to creating agile and versatile locomotion planners. To this end, models and tools have been designed to predict CoM behavior in robots and humans.

Various approaches have been used to estimate the CoM in robots. Previous studies [1]–[3] employed a forward kinematics or a ZMP [4] based computation approach for CoM state estimation. Such estimators proved accurate for modeling CoM position, but required continuous body link attitude and force sensor information. To further improve the accuracy of the forward kinematics paradigm, the authors in [5] presented a novel Kalman filter for CoM estimation based on a three scheme hybrid approach, and in [6] [7] the CoM position was estimated using spectral analysis to filter

multi-sensor data. However, the drawback to these methods remained their continued reliance on expensive inertial and force sensors for CoM estimation.

Similar issues have plagued CoM estimation in humans. The body segmental method based on data from anthropomorphic tables [8]–[10] is a standard technique. Nevertheless, it requires constant body marker tracking and video data to perform CoM position approximation. Newtonian techniques that use ground reaction forces have also been used. The authors in [11] [12] attached force platforms to the terrain and in [13] they were attached directly to footwear. But such data acquisition methods are clumsy and impractical outside of laboratory settings.

In recent years the statically equivalent serial chain(SESC) method first developed in [14] has been further refined in [15] [16] to limit the usage of external sensors for human CoM estimation. The method represents a polyarticulated system as a branched multi-link chain with the CoM position of the body specified by the end-effector of the chain. In order to obtain subject specific data and obviate dependence on force recordings, subjects undergo an extended calibration phase during which stable postures and sizable force readings and motion capture data are combined to determine the SESC for the subject. Next, sensor devices are employed to find the joint measurements from which the instantaneous CoM position can be calculated. Naturally, real-time joint measurement is a non-trivial task. To facilitate this operation the authors of [17] [18] switched to a Wii balance board and Kinect for force and video data. Needless to say, serious questions anent device cost and manageability remain, and in general, dependence on expensive and intrusive equipment continues to impede CoM estimation in all but controlled and non-realistic laboratory settings.

This paper presents a geometric approach for CoM position estimation characterized as non-onerous and bereft of dependence on video or force data. The inspiration behind the geometric approach is the concept that the environment and the architecture of the kinematic body work in tandem to impose limitations on the possible CoM positions in the terrain [19]. Thus, knowledge of the terrain, body kinematic constraints, and foot contact locations, provides insightful information that allows for accurate CoM position estimation. This paper is organized as follows: Section II outlines the overall framework and presents descriptions of the key components. Section III explains generation of the entire CoM path through the terrain. Finally, in Section IV, human motion capture data are used for validation and comparisons are made with CoM position and phase space trajectories.

II. FRAMEWORK OVERVIEW

The geometric approach develops natural walking CoM position estimates over irregular planar terrains (Fig. 2) using the following steps: (1) knowledge of the terrain, desired step durations and foot contact locations enable creation of intermediary *virtual steps*, which are imaginary steps present in the environment that describe CoM behavior during double support phases. (2) The desired real foot contact locations, virtual steps, and terrain geometry are utilized to calculate apex angles. Apex angles describe the CoM direction of motion as the CoM passes directly above both real and virtual steps. (3) Using subject specific kinematic constraints, OGH curves having minimum curvature (MC) and strain energy (SE) trace out the full CoM position path. The path is constructed incrementally using the step (virtual and real) locations and the apex angles. The final CoM position path is then formed by joining all the piecewise OGH segments.

A. Virtual Steps

Virtual steps define nonphysical reference points in the environment that capture CoM behavior between successive foot locations. The concept is drawn from observing that performance of successive steps by a subject results in CoM position displacement in the negative vertical direction relative to the standing upright position. This vertical displacement Δ_{com_z} allows for accurate description of CoM behavior between consecutive foot centers of pressure (CoP). Hence, virtual steps are defined as follows: a virtual step is a point in space (x_{vs}, z_{vs}) whose location lies between successive foot contact locations and whose value can be computed directly using adjoining real CoP locations. This paper adopts a geometric approach to virtual step calculation and regards the center of the hip joint and sequential CoP locations as forming three points of a changing and moving isosceles triangle. Under such a model, the displacement Δ_{com_z} can be found directly by considering the height h of the changing triangle. A geometric representation of this model is given in Fig. 1 with b defined as the length of the leg, d as the distance taken from the subject's standing upright CoM to the hip joint center as provided in [8] [10], and a as the sagittal distance between adjacent CoPs. Thus, two adjacent CoPs (x_{cop_i}, z_{cop_i}) and (x_{cop_j}, z_{cop_j}) determine the vertical CoM displacement $\Delta_{com_z}^{ij}$ as follows:

$$\Delta_{com_z}^{ij} = (b + d) - (h_{ij} + d) \quad (1)$$

and after expansion of terms

$$\Delta_{com_z}^{ij} = b - \sqrt{b^2 - \frac{(x_{cop_j} - x_{cop_i})^2}{4}} \quad (2)$$

Lastly, the vertical component z_{vs}^i of the i th virtual step is chosen as

$$z_{vs}^i = \min(z_{cop_i}, z_{cop_j}) - \Delta_{com_z}^{ij} \quad (3)$$

Note that $\Delta_{com_z}^{ij}$ is always specified with respect to sagittal CoP locations (Equation 2). By treating the leg configuration

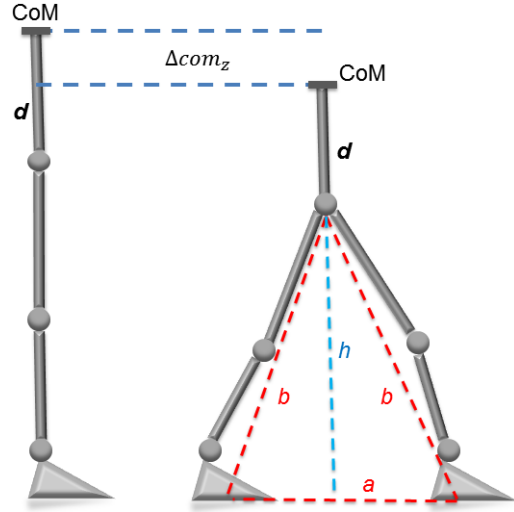


Fig. 1: Sagittal plane view showing step geometric model.

as constant during double support phases (Fig 1), this obviates the need for real-time joint kinematic tracking and simplifies the model considerably.

The horizontal component value x_{vs}^i is computed by considering adjacent CoP height differences as well as desired step durations. These factors were observed to exercise the greatest influence on the sagittal location of the dip x_{vs}^i . For two consecutive CoP locations (x_{cop_i}, z_{cop_i}) and (x_{cop_j}, z_{cop_j}) with desired step durations Δt_i and Δt_j , the height and time proportions of x_{vs}^i are defined as

$$T = \frac{\max(\Delta t_i, \Delta t_j)}{\Delta t_i + \Delta t_j} \quad (4)$$

$$H = \sqrt{\frac{\left(\frac{x_{cop_j} - x_{cop_i}}{2}\right)^2 + (z_{cop_j} - z_{cop_i})^2}{(x_{cop_j} - x_{cop_i})^2 + (z_{cop_j} - z_{cop_i})^2}} \quad (5)$$

where T is a step duration bias and H is the geometric hypotenuse ratio of step CoPs that characterizes height influence. Next, the weighted sum of the height and time proportions is used to determine a horizontal offset Δ_x^{ij}

$$\Delta_x^{ij} = |x_{cop_i} - x_{cop_j}| \left(\frac{T + H}{2} \right) \quad (6)$$

which is the sagittal displacement value. Finally, x_{vs}^i is found by assigning Δ_x^{ij} to the CoP of greater step duration.

$$x_{vs}^i = \begin{cases} x_{cop_i} + \Delta_x^{ij} & \text{if } \Delta t_i \geq \Delta t_j \\ x_{cop_j} - \Delta_x^{ij} & \text{if } \Delta t_i < \Delta t_j \end{cases} \quad (7)$$

Hence, locations of virtual steps always lie between sequential CoPs while possessing vertical values z_{vs}^i that lie below $\min(z_{cop_i}, z_{cop_j})$.

B. Apex Angles

Apex angles describe the behavior of the CoM directly above virtual and real step locations. Determination of the angles is found by observing that steps undertaken in the

terrain strongly influence the behavior of the CoM at both the current and following step, for example, walking up a flight of stairs. As such, apex angles must be computable based on the locations of the previous and next step locations. This is achieved by computing the arctan angle between steps. Generally speaking, virtual step apex angles are derived based on the anterior step CoP and real step apex angles depend on the location and influence of the forward step CoP. Algorithm 1 presents the full procedure for finding apex angles while Fig. 2 displays a terrain example along with foot CoPs, virtual steps, and apex angles.

Algorithm 1: Apex Angles

Input: Let $S=\{1\dots n\}$ be the steps with S odd being real steps and S even the virtual steps.

$\psi_{ij} \leftarrow \text{atan2d}$ angle from step (x_i, z_i) to (x_j, z_j) .

$\theta_i \leftarrow$ apex angle of each step.

Initial angle θ_1 for $S=\{1\}$ is defined as

$$\theta_1 = \begin{cases} \max(|\psi_{12}|, |\psi_{13}|) & \text{if } z_3 \geq z_1 \\ \min(|\psi_{12}|, |\psi_{13}|) & \text{if } z_3 < z_1 \end{cases}$$

for $i = 2$ to n **do**

if $S=\{i\}$ is a virtual step **then**

$\theta_i = \psi_{i-1,i}$

else {the step is real}

$$\theta_i = \begin{cases} \max(\psi_{i-1,i}, \psi_{i,i+2}) & \text{if } z_{i+2} \geq z_i \\ \psi_{i-1,i} & \text{if } z_{i+2} < z_i \end{cases}$$

end if

end for

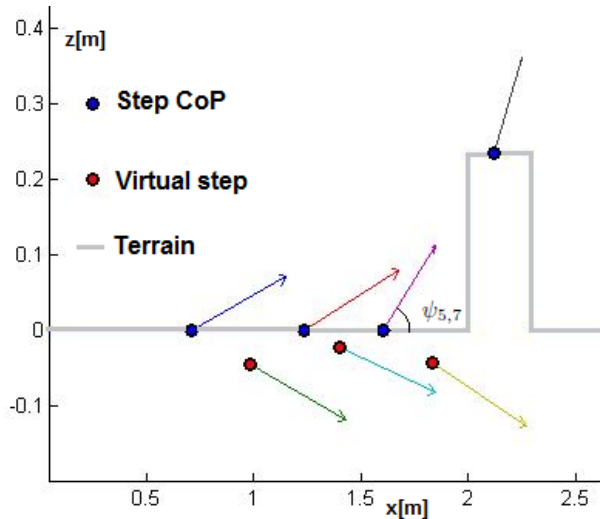


Fig. 2. A walking sequence consisting of four real steps. Virtual step locations and apex angles(vectors) also depicted.

C. Optimized geometric Hermite curve

In this work OGH curves optimized for MC are used to construct CoM position estimates over the terrain. An OGH curve is a cubic spline composed of piecewise segments

each described in Hermite form [20]. OGH curves having MC provide a natural choice for CoM position estimation because they allow for curve generation through specification of the endpoint tangent vectors and produce curves that are mathematically smooth and devoid of extreme behavior.

Definition 1. Given two endpoints P_0 and P_1 , and two endpoint tangent vectors V_0 and V_1 , a cubic polynomial curve $P(t)$, $t \in [t_0, t_1]$, is called an optimized geometric Hermite(OGH) curve with respect to the endpoint conditions P_0, P_1, V_0, V_1 if it has the smallest curvature variation among all cubic Hermite curves $\bar{P}(t)$, $t \in [t_0, t_1]$ satisfying the following condition:

$$\bar{P}(t_0) = P_0, \bar{P}(t_1) = P_1, \bar{P}'(t_0) = \alpha_0 V_0, \bar{P}'(t_1) = \alpha_1 V_1 \quad (8)$$

where α_0 and α_1 are arbitrary real numbers, and the cubic Hermite curve $\bar{P}(t)$, $t \in [t_0, t_1]$ satisfying the constraints in (8) can be expressed as

$$\bar{P}(t) = (2s+1)(s-1)^2 P_0 + (-2s+3)s^2 P_1 + (1-s)^2 s (t_1 - t_0) \alpha_0 V_0 + (s-1)s^2 (t_1 - t_0) \alpha_1 V_1 \quad (9)$$

where $s = (t - t_0)/(t_1 - t_0)$. The objective function to optimize is defined as

$$E = \int_{t_0}^{t_1} [\bar{P}'''(t)]^2 dt \quad (10)$$

and is the approximate curvature variation of the curve $\bar{P}(t)$.

Tangent vectors V_0, V_1 are defined using tangent angles θ and ϕ respectively, with θ the counterclockwise angle from $\bar{P}_0\bar{P}_1$ to V_0 , and ϕ the counterclockwise angle from $\bar{P}_0\bar{P}_1$ to V_1 . The tangent angle inputs treated here are taken as the apex angles previously discussed. The usage of apex angles generates OGH curves with MC that capture the CoM direction of motion reliably. Thus, curves are produced that ensure fidelity to the step locations as well as the step-to-step CoM behavior across the terrain. Further details anent tangent angles and OGH curves are given in [20].

III. CoM PATH CONSTRUCTION

Broadly speaking, the following procedure is used to produce CoM estimates. 1) Two apex angles and step locations produce a family of OGH curves with MC. The curves must meet the subject's kinematic constraints. 2) The curve with minimum (SE) among all curves generated is chosen as the path and forms the start location for the following step. 3) The next apex angle and step location is processed. The above procedure continues until the last step is reached.

The subject's kinematic constraints are abstracted in this work as a vertical displacement range $\{(z_{min} + k, z_{max} + k) | (z_{min} + k) \leq p_{com_z} \leq (z_{max} + k)\}$, which specifies the range of viable CoM positions for the subject at terrain height k . Note that the range is discretized by 0.01m for efficiency and that k is simply the vertical component, z_i , of step placement (x_i, z_i) . This abstraction allows for representation of human/robot kinematic variation and generates paths that account for the unique limitations of a body. Furthermore, because only irregular planar terrains are treated in this work $(z_{min} + k, z_{max} + k)$ are terrain dependent such that $\forall p_{ter_z} \in \mathbb{R} : |(z_{min} + k) - p_{ter_z}| = c$, with p_{ter_z} being the terrain's vertical position and where c is a constant. This

places a lower bound on possible CoM positions determined by the body’s kinematic constraints. Thus, CoM paths are created that are faithful to the body’s motion over the terrain.

In the case of human subjects, approximate values for z_{min} and z_{max} are taken from body anthropomorphic data. Given a subject’s stature, z_{min} is approximated as the vertical CoM location while executing a lunge, and z_{max} as the standing upright CoM position including the distance from the foot’s heel to the ball. In this manner, accurate approximations for z_{min} and z_{max} specific to a subject can be obtained using only stature and anthropomorphic data [8] [21]. The complete algorithm for CoM construction is provided in Algorithm 2 while an example is given in Fig. 3.

Algorithm 2: CoM Path Construction

Input:

Steps $S = \{(x_1, z_1) \dots (x_n, z_n)\}$

Apex angles $\{\theta_1 \dots \theta_n\}$

Constraints z_{min} and z_{max}

Initial CoM position $(x_1, p_{com_z_init})$

for $i = 2$ to n **do**

for $p_{com_z} = (z_{min} + z_i)$ to $(z_{max} + z_i)$ **do**

1. Generate OGH curve with minimum curvature using $(x_1, p_{com_z_init})$, θ_1 to (x_i, p_{com_z}) , θ_i
2. If OGH curve violates CoM lower bound threshold, reject curve
3. $p_{com_z} = p_{com_z} + 0.01m$

end for

- a. Select endpoint (x_i, p_{com_z}) corresponding to curve G_ℓ with minimum (SE) among all curves generated.
- b. Set CoM path to G_ℓ
- c. $x_1 = x_i$, $p_{com_z_init} = p_{com_z}$, $\theta_1 = \theta_i$

end for

return Complete CoM path, the piecewise composition of each curve G_ℓ .

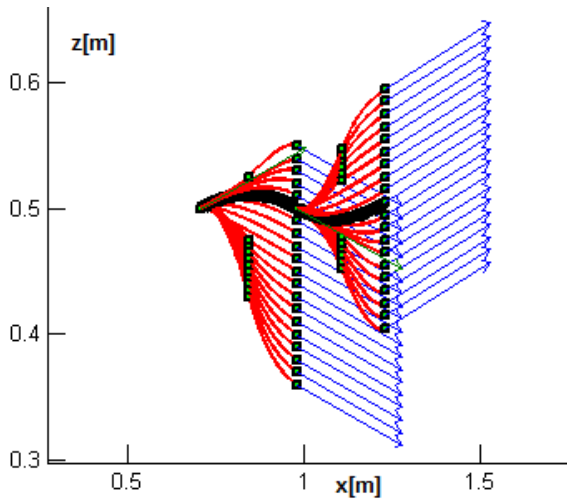


Fig. 3. Family of OGH curves with MC(red) for three steps and apex angles of Fig. 2. At each iteration, the OGH curve having the minimum (SE) is chosen as the path(black).

IV. EXPERIMENTAL RESULTS

A. Experimental Setup and Data Collected

Two terrains composed of obstacles of variable heights were each navigated by 6 different subjects. Motion capture video data was gathered for each traversal and analyzed using Matlab. To minimize lens distortion and obtain unadulterated planar motion, the camera was placed at a sufficiently far distance from the human traversal motion. The raw video was shot at 30 frames per second but only every 3rd frame was used to decrease data processing. A vectorial weighted sum using 14 body segment CoM locations and relative masses [8] was used to calculate the CoM position for each trial run. Body segment markers were placed: one for the head(head and neck), one for the torso(chest, abdomen and pelvis), and one on each foot, calf, thigh, hand, forearm and upper arm. The resulting data was interpreted using Matlab and a curve fit produced using the cftool. Each step’s contact support point p_{cop_k} was acquired from the video using Matlab’s ginput function and estimated initially as the surface midpoint of the contact foot location. The duration of each step was acquired directly from the raw video while terrain geometry information was provided as input to the system. An example traversal is shown in Fig. 4. while subject attributes are described in Table I.

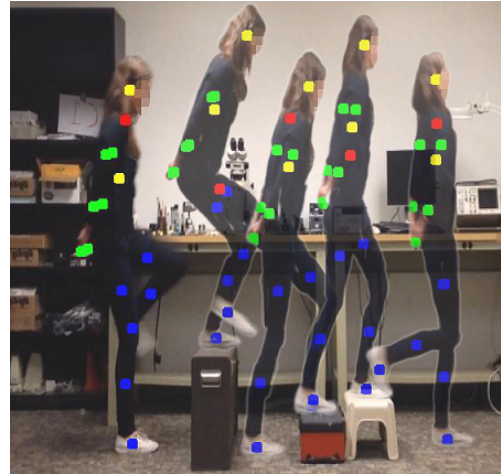


Fig. 4. Snapshots of sagittal human traversal motion over terrain.

TABLE I:
Subject Attributes Data.

Subject	Gender	Height	Weight
1	M	1.75m	68kg
2	M	1.75m	84kg
3	M	1.78m	82kg
4	M	1.72m	75kg
5	F	1.73m	56kg
6	F	1.55m	41kg

B. Cross-validation

The geometric approach was used to generate CoM position estimates for all subjects on both terrains and then

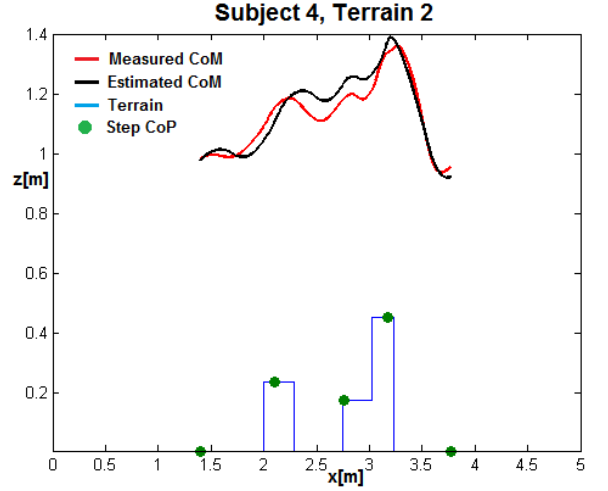
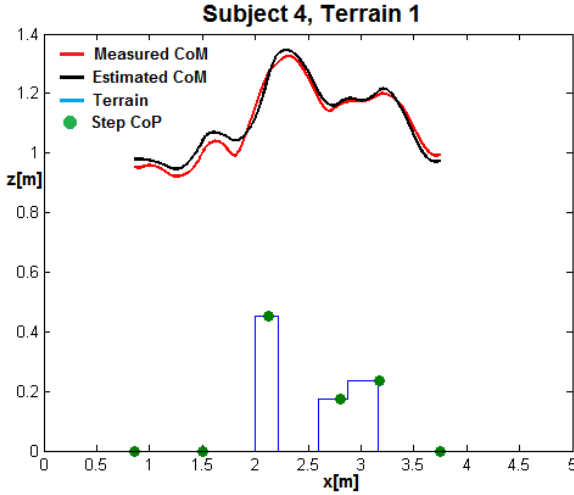


Fig. 5: Subject 4: (Left) a six step walking sequence over terrain 1. (Right) a five step walking sequence over terrain 2. The estimated versus measured CoM vertical position rmse is 0.0244m and 0.0405m respectively.

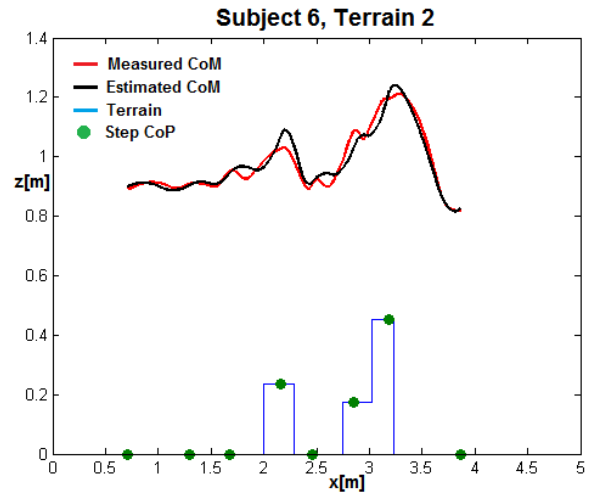
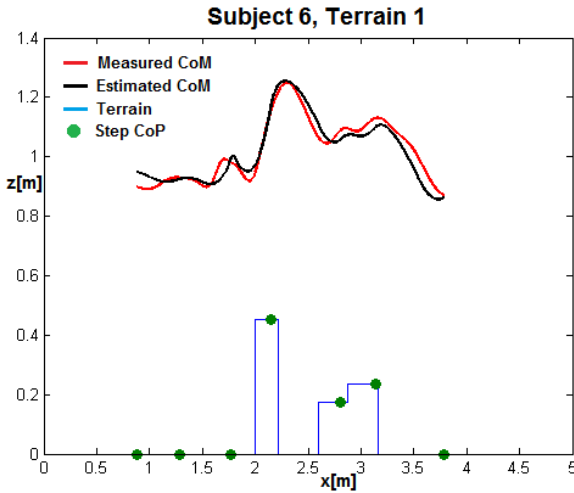


Fig. 6: Subject 6: (Left) a seven step walking sequence over terrain 1. (Right) an eight step walking sequence over terrain 2. The estimated versus measured CoM vertical position rmse is 0.0307m and 0.0252m respectively.

compared with CoM data obtained using motion capture video. The automatically generated curves included an x -direction adjustment of $\pm 5\text{cm}$ to p_{cop_k} . This attunement resulted in more accurate correlation with the observed data and provides a reasonable adjustment bearing in mind the physical limitations of the foot and ankle. Foot geometry and ankle use prevent true human point contact behavior and perpetually shift the CoP. This disallows measurement of p_{cop_k} using only our video technique and justifies small adjustments to the initial estimate. The CoM paths using motion capture(measured) and geometric approach(estimated) for 2 subjects traversing terrains 1 and 2 are shown in Fig. 5 and 6. Additionally, the root mean squared error(rmse) between the vertical CoM position (measured versus estimated) for all twelve runs is reported in Table II. The subjects averaged a rmse of 0.0333m on terrain 1, while for terrain 2, the

TABLE II:
RMSE Est. vs Measured CoM Vertical Position

Subject	Terrain 1	Terrain 2
1	0.0229m	0.0401m
2	0.0273m	0.0306m
3	0.0579m	0.0444m
4	0.0244m	0.0405m
5	0.0364m	0.0273m
6	0.0307m	0.0252m
avg rmse	0.0333m	0.0347m

average rmse was 0.0347m. The results indicate an average performance across both terrains and for all subjects that is approximately similar in value. This result is both remarkable and encouraging given the large disparity of subject heights, weights, and step sequences(e.g., the 6 step walking sequence

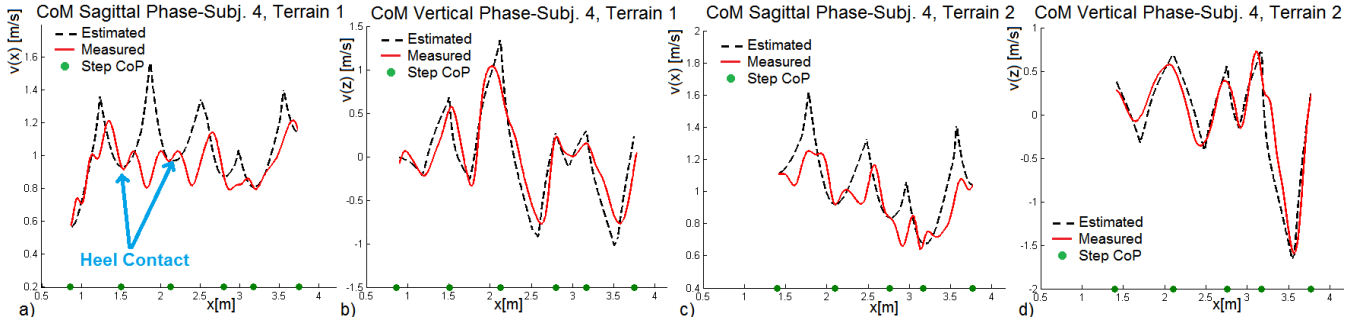


Fig. 7: Subject 4 sagittal and vertical phase curves using CoM estimate for terrain 1(a and b) and 2(c and d) from Fig 5.

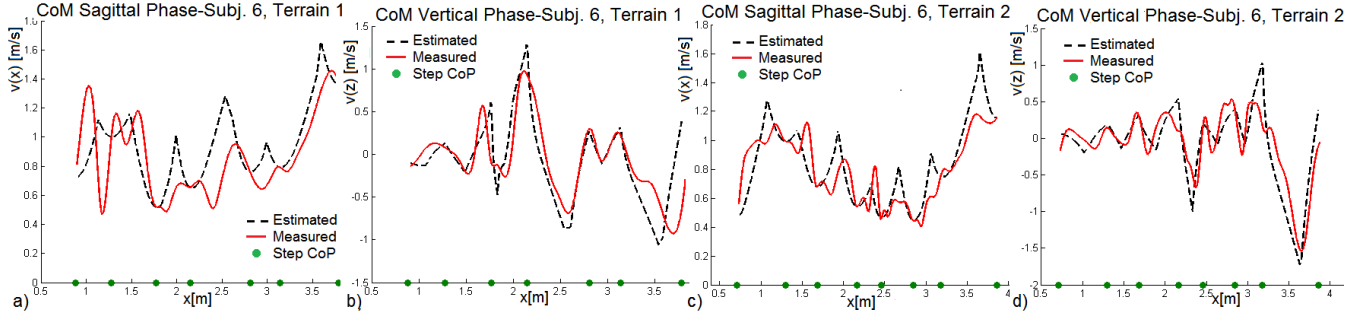


Fig. 8: Subject 6 sagittal and vertical phase curves using CoM estimate for terrain 1(a and b) and 2(c and d) from Fig 6.

shown in Fig. 5(left) and the 7 step walking sequence shown in Fig. 6(left)). Moreover, the generated CoM estimates always displayed the same CoM pattern of behavior observed in the real world including in cases having a relatively poor rmse, for example 0.0405m as shown in Fig. 5(right). In general, the results exhibit significant correlation between the measured and estimated CoM positions and demonstrate the method’s ability to encapsulate vital kinematic and terrain information to produce accurate CoM estimates.

C. CoM State-Space Behavior

For further analysis of the correspondence between the measured and estimated CoM paths, state-space trajectory comparisons were performed. The human traversal sagittal and vertical phase trajectories were extracted directly from the human traversal videos. State-space trajectories for the geometric approach were produced using the numerical integration technique outlined in [22]–[24]. The numerical integration technique uses perturbation theory to predict CoM phase curves in the neighborhood of step contact locations using a desired kinematic CoM path. The kinematic CoM path used here is the automatically generated path produced by the geometric approach. This allows for confirmation that the CoM estimate generated by the geometric approach produces approximately similar CoM state-space behavior as that obtained using video motion capture, and for validation that the automatic step CoPs, p_{cop_k} , match the real step locations of the human subject. Phase curves using the measured and estimated CoM paths from Fig. 5 and 6 are shown in Fig. 7 and 8. Note that for clarity of presentation, the step CoPs were included along the x-axis.

As can be seen, the results display significant correlation of phase curves between the human and artificial CoM phase portraits, supporting the CoM path estimates produced by the geometric approach. Interestingly, p_{cop_k} also matches the real step locations as observed in Fig. 7(a) where p_{cop_k} coincides with the heel contact point. The measured phase curve (red) then decelerates, creating a valley as the subject’s weight shifts towards the front of the foot. The same pattern occurs again when the next step is taken. This behavior is shown for two steps in Fig. 7(a) with blue arrows. Similar behavior is observed in the sagittal phase curves for all subjects.

Lastly, it is important to highlight the alignment between the real and geometric step CoP locations used. Specifically, the geometric estimates produced approximately match the observed real world results and it is not the case that CoM estimates and phase curves were generated using vastly different values for p_{cop_k} . Rather, the geometric CoM estimates produced are derived using approximate real world step CoP locations. Ergo, the geometric approach can be used as a predictive model for CoM behavior estimation using terrain geometry and subject height information, and desired step CoP locations. This provides a reliable and less cumbersome approach that greatly facilitates the study CoM dynamics in irregular planar terrains.

V. DISCUSSION AND FUTURE WORK

The work presented in this paper offered an innovative geometric approach to estimate CoM position in irregular planar terrains for natural walking motion that is independent of force or video sensors. The approach provides reliable CoM estimation that accurately describes natural walking

behavior using only essential terrain geometry and body kinematic information.

The geometric approach provides several important advantages including: 1) independence from expensive and time prohibitive sensor equipment 2) accurate CoM estimation and state-space trajectories that accounts for variations in subject kinematic constraints and 3) the ability to handle irregular planar environments. These benefits render the approach versatile and dependable to use in non-laboratory settings.

Comparisons with human traversal data were performed and yielded small rmse, however, further work could improve the accuracy of the approach. In particular, extensions to wider subject weight distributions should be studied to explore their effect on CoM paths. Larger varieties of terrains could be investigated as well, including extensions to 3D environments and CoM behavior estimation in the lateral direction. These advancements could lead to more versatility and increase the generalization of the approach.

REFERENCES

- [1] B. J. Stephens, "State estimation for force-controlled humanoid balance using simple models in the presence of modeling error," in *Robotics and Automation (ICRA), 2011 IEEE International Conference on*. IEEE, 2011, pp. 3994–3999.
- [2] H. Dai, A. Valenzuela, and R. Tedrake, "Whole-body motion planning with centroidal dynamics and full kinematics," in *Humanoid Robots (Humanoids), 2014 14th IEEE-RAS International Conference on*. IEEE, 2014, pp. 295–302.
- [3] C. G. Atkeson *et al.*, "State estimation of a walking humanoid robot," in *Intelligent Robots and Systems (IROS), 2012 IEEE/RSJ International Conference on*. IEEE, 2012, pp. 3693–3699.
- [4] G. G. Muscolo, C. T. Recchiuto, C. Laschi, P. Dario, K. Hashimoto, and A. Takanishi, "A method for the calculation of the effective center of mass of humanoid robots," in *Humanoid Robots (Humanoids), 2011 11th IEEE-RAS International Conference on*. IEEE, 2011, pp. 371–376.
- [5] K. Masuya and T. Sugihara, "Com motion estimation of a humanoid robot based on a fusion of dynamics and kinematics information," in *Intelligent Robots and Systems (IROS), 2015 IEEE/RSJ International Conference on*. IEEE, 2015, pp. 3975–3980.
- [6] J. Carpentier, M. Benallegue, N. Mansard, and J.-P. Laumond, "Center of mass estimation for polyarticulated system in contact—a spectral approach," 2015.
- [7] —, "A kinematics-dynamics based estimator of the center of mass position for anthropomorphic system. a complementary filtering approach," in *Humanoid Robots (Humanoids), 2015 IEEE-RAS 15th International Conference on*. IEEE, 2015, pp. 1121–1126.
- [8] D. A. Winter, *Biomechanics and motor control of human movement*. John Wiley & Sons, 2009.
- [9] V. Zatsiorsky and V. Seluyanov, "The mass and inertia characteristics of the main segments of the human body," *Biomechanics viii-b*, vol. 56, no. 2, pp. 1152–1159, 1983.
- [10] P. De Leva, "Adjustments to zatsiorsky-seluyanov's segment inertia parameters," *Journal of biomechanics*, vol. 29, no. 9, pp. 1223–1230, 1996.
- [11] T. Shimba, "An estimation of center of gravity from force platform data," *Journal of Biomechanics*, vol. 17, no. 1, pp. 53–60, 1984.
- [12] D. L. King and V. M. Zatsiorsky, "Extracting gravity line displacement from stabilographic recordings," *Gait & Posture*, vol. 6, no. 1, pp. 27–38, 1997.
- [13] H. M. Schepers, E. H. Van Asseldonk, J. H. Buurke, and P. H. Veltink, "Ambulatory estimation of center of mass displacement during walking," *Biomedical Engineering, IEEE Transactions on*, vol. 56, no. 4, pp. 1189–1195, 2009.
- [14] B. Espiau and R. Boulic, "On the computation and control of the mass center of articulated chains," 1998.
- [15] S. Cotton, A. P. Murray, and P. Fraitse, "Estimation of the center of mass: from humanoid robots to human beings," *Mechatronics, IEEE/ASME Transactions on*, vol. 14, no. 6, pp. 707–712, 2009.
- [16] S. Cotton, M. Vanoncini, P. Fraitse, N. Ramdani, E. Demircan, A. Murray, and T. Keller, "Estimation of the centre of mass from motion capture and force plate recordings: a study on the elderly," *Applied Bionics and Biomechanics*, vol. 8, no. 1, pp. 67–84, 2011.
- [17] A. González, M. Hayashibe, and P. Fraitse, "Estimation of the center of mass with kinect and wii balance board," in *Intelligent Robots and Systems (IROS), 2012 IEEE/RSJ International Conference on*. IEEE, 2012, pp. 1023–1028.
- [18] A. González, M. Hayashibe, V. Bonnet, and P. Fraitse, "Whole body center of mass estimation with portable sensors: Using the statically equivalent serial chain and a kinect," *Sensors*, vol. 14, no. 9, pp. 16955–16971, 2014.
- [19] L. Barrios and W.-M. Shen, "Phase space planning and optimization of foot placements in rough planar terrains," in *Robotics and Automation (ICRA), 2015 IEEE International Conference on*. IEEE, 2015, pp. 3582–3589.
- [20] J. Chi, C. Zhang, and L. Xu, "Constructing geometric hermite curve with minimum curvature variation," in *9th International Conference on Computer Aided Design and Computer Graphics*. IEEE, 2005, pp. 58–66.
- [21] R. Contini, "Body segment parameters. ii," *Artificial limbs*, vol. 16, no. 1, p. 1, 1972.
- [22] L. Sentis and B. Fernandez, "Perturbation theory to plan dynamic locomotion in very rough terrains," in *Intelligent Robots and Systems (IROS), 2011 IEEE/RSJ International Conference on*. IEEE, 2011, pp. 2267–2273.
- [23] L. Sentis and M. Slovic, "Motion planning of extreme locomotion maneuvers using multi-contact dynamics and numerical integration," in *Humanoid Robots (Humanoids), 2011 11th IEEE-RAS International Conference on*. IEEE, 2011, pp. 760–767.
- [24] L. Sentis, B. Fernandez, and M. Slovic, "Prediction and planning methods of bipedal dynamic locomotion over very rough terrains," in *The International Symposium of Robotics Research*, 2011.